

Symmetries and Angular Scattering Properties of Metasurfaces

K. Achouri¹ and O. J. F. Martin¹

¹Nanophotonics and Metrology Laboratory, Department of Microengineering, École Polytechnique Fédérale de Lausanne (EPFL), Route Cantonale, 1015 Lausanne, Switzerland
karim.achouri@epfl.ch

Abstract – We study the angular scattering behavior of bianisotropic metasurfaces and deduce relationships between the corresponding symmetrical angular scattering properties and the structural symmetries of their scattering particles. This may be of practical interest for the realization of metasurfaces with complex angular scattering characteristics.

I. INTRODUCTION

Over the past few years, we have extensively worked on the modelling of electromagnetic metasurfaces and have hence developed a general synthesis and analysis framework based on the generalized sheet transition conditions (GSTC) [1–4]. This framework models a metasurface as a zero-thickness sheet and relates its bianisotropic susceptibilities to the fields that interact with it.

The purpose of the present work [5] is: 1) to clarify the relationship between the presence of certain susceptibilities, such as those responsible for the excitation of normal polarizations, and the angular scattering behavior of metasurfaces, and 2) to relate the presence of these susceptibilities to the geometry of the metasurface scattering particles.

II. SYMMETRIES AND ANGULAR SCATTERING

Consider a metasurface lying in the xy -plane at $z = 0$, the corresponding GSTC read

$$\hat{z} \times \Delta \mathbf{H} = j\omega \mathbf{P} - \hat{z} \times \nabla M_z, \quad (1a)$$

$$\hat{z} \times \Delta \mathbf{E} = -j\omega\mu_0 \mathbf{M} - \frac{1}{\epsilon_0} \hat{z} \times \nabla P_z, \quad (1b)$$

where Δ refers to the difference of the fields on both sides of the metasurface, and \mathbf{P} and \mathbf{M} are the electric and magnetic polarization densities, respectively. In the general case of a bianisotropic metasurface, these polarization densities are given in terms of the average fields by

$$\mathbf{P} = \epsilon_0 \bar{\chi}_{ee} \cdot \mathbf{E}_{av} + \epsilon_0 \eta_0 \bar{\chi}_{em} \cdot \mathbf{H}_{av}, \quad (2a)$$

$$\mathbf{M} = \bar{\chi}_{mm} \cdot \mathbf{H}_{av} + \frac{1}{\eta_0} \bar{\chi}_{me} \cdot \mathbf{E}_{av}, \quad (2b)$$

where $\bar{\chi}_{ee}$, $\bar{\chi}_{mm}$, $\bar{\chi}_{em}$ and $\bar{\chi}_{me}$ are the electric, magnetic, magnetic-to-electric and electric-to-magnetic susceptibility tensors, respectively.

In order to assess the angular scattering behavior of a metasurface, we compute its scattering parameters for an arbitrary incidence angle θ . Here, we assume that the metasurface is spatially uniform and that it hence scatters electromagnetic waves according to Snell law. We consider the situation depicted in Fig. 1, where the numbers 1 to 4 correspond to input/output ports. For simplicity but without loss of generality, we assume only TM polarization throughout. The metasurface angular scattering parameters may be computed by first specifying the difference and average fields in (1) and (2), and then solving for amplitude of the reflected (R) and transmitted (T) waves. Accordingly, the difference of the fields are, at $z = 0$, given by

$$\Delta \mathbf{E} = \pm \hat{x} \frac{k_z}{k} (1 + R - T), \quad \Delta \mathbf{H} = \hat{y} \frac{1}{\eta_0} (-1 + R + T), \quad (3)$$

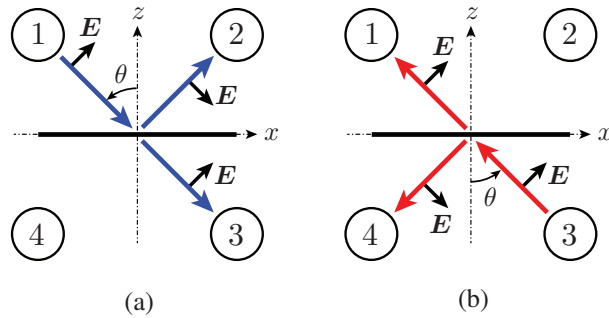


Fig. 1: Incidence angle and field polarization for (a) downward wave incidence and (b) an upward wave incidence.

and the average fields are given by

$$E_{x,av} = \frac{k_z}{2k} (1 + T + R), \quad E_{z,av} = \frac{k_x}{2k} (1 + T - R), \quad H_{y,av} = \mp \frac{1}{2\eta_0} (1 + T - R), \quad (4)$$

where $k_z = k \cos \theta$ and $k_x = k \sin \theta$ and where we have dropped the term $e^{-jk_x x}$ for conciseness. In these

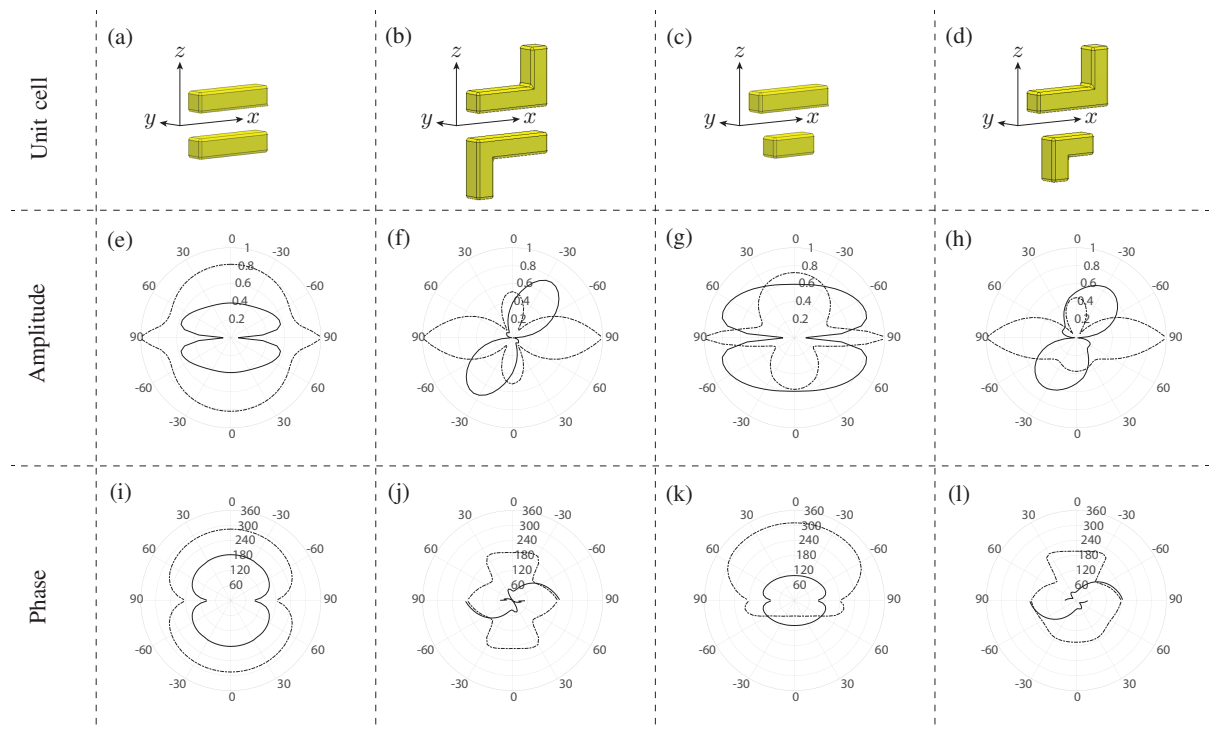


Fig. 2: Angular scattering properties of 4 different reciprocal metasurfaces. Top row, metasurface unit cells which are periodically arranged in the xy -plane with a square lattice period of 200 nm to form the corresponding metasurfaces. Middle row, amplitude of the transmission (solid lines) and reflection (dashed-dotted lines) coefficients versus incidence angle. Note that the angular coordinate of these plots corresponds to the incidence angle θ following the convention adopted in Figs. 1a and 1b. Bottom row, phase of the transmission and reflection coefficients. The unit cells in (a) and (c) have been simulated at $\lambda_0 = 600$ nm, while the unit cells (b) and (d) have been simulated at $\lambda_0 = 660$ nm.

equations, the top signs correspond to incident wave excitation propagating backward along z , as in Fig. 1a, while the bottom signs correspond to incident waves propagating forward as in Fig. 1b. The resulting scattering

parameters are

$$R = \frac{2}{C_2} \{ k_x^2 \chi_{ee}^{zz} - k_z^2 \chi_{ee}^{xx} - k_z [k_x (\chi_{ee}^{xz} - \chi_{ee}^{zx}) \mp k (\chi_{em}^{xy} - \chi_{me}^{yx})] \mp k k_x (\chi_{em}^{zy} + \chi_{me}^{yz}) + k^2 \chi_{mm}^{yy} \}. \quad (5a)$$

$$T = \frac{j k_z}{C_2} \{ k_x^2 (\chi_{ee}^{xz} \chi_{ee}^{zx} - \chi_{ee}^{xx} \chi_{ee}^{zz}) + (2j \mp k \chi_{em}^{xy})(2j \mp k \chi_{me}^{yx}) + k_x [\chi_{ee}^{zx} (2j \mp k \chi_{em}^{xy}) + \chi_{ee}^{xz} (2j \mp k \chi_{me}^{yx}) \pm k \chi_{ee}^{xx} (\chi_{em}^{zy} + \chi_{me}^{yz})] - k^2 \chi_{ee}^{xx} \chi_{mm}^{yy} \}. \quad (5b)$$

$$C_2 = 2 [k_z^2 \chi_{ee}^{xx} + k_x^2 \chi_{ee}^{zz} \mp k k_x (\chi_{em}^{zy} + \chi_{me}^{yz}) + k^2 \chi_{mm}^{yy}] \pm k^2 (\chi_{ee}^{xx} \chi_{mm}^{yy} - \chi_{em}^{xy} \chi_{me}^{yx}) - j k_z [k_x^2 (\chi_{ee}^{xz} \chi_{ee}^{zx} - \chi_{ee}^{xx} \chi_{ee}^{zz}) + 4 \mp k k_x (\chi_{ee}^{xz} \chi_{em}^{xy} + \chi_{ee}^{zx} \chi_{me}^{yx} - \chi_{ee}^{xx} (\chi_{em}^{zy} + \chi_{me}^{yz}))]. \quad (5c)$$

From these expressions, we may straightforwardly deduce the angular scattering behavior of a metasurface. For instance, we note that all susceptibilities linearly related to k_z are responsible for asymmetric scattering with respect to the z -axis.

In order to relate the angular scattering, the presence of certain susceptibilities and the geometry of the scattering particles altogether, we have performed full-wave simulations of scattering particles with simple geometries (simple metallic rods with a length of about 100 nm) and extracted their corresponding scattering parameters in terms of the incidence angle θ . The results are presented in Fig. 2. Comparing the symmetries associated with the particles geometry and the corresponding scattering plots in Fig. 2, we obtain the relationships summarized in Table 1.

| Type | Reflection | Transmission | Structure |
|--|----------------|----------------|------------------------------------|
| Birefringent $\chi_{ee}^{xx}, \chi_{mm}^{yy}$ | $C_2 \sigma_z$ | $C_2 \sigma_z$ | $C_2 \sigma_z$ (or σ_x) |
| Anisotropic $\chi_{ee}^{xx}, \chi_{mm}^{yy}$ $\chi_{ee}^{xz}, \chi_{ee}^{zx}, \chi_{ee}^{zz}$ | $C_2 \sigma_z$ | C_2 | C_2 |
| Bianisotropic $\chi_{ee}^{xx}, \chi_{mm}^{yy}$ $\chi_{em}^{xy}, \chi_{me}^{yx}$ | σ_z | $C_2 \sigma_z$ | σ_z |
| Bianisotropic $\chi_{ee}^{xx}, \chi_{mm}^{yy}, \chi_{ee}^{zz}$ $\chi_{ee}^{xz}, \chi_{ee}^{zx}, \chi_{em}^{xy},$ $\chi_{me}^{yx}, \chi_{em}^{zy}, \chi_{me}^{yz}$ | σ_z | C_2 | — |

Table 1: Symmetry relationships between angular scattering and unit cell structure for the 4 types of reciprocal metasurfaces in Fig. 2. C_2 refers to a 2-fold (180°) rotation symmetry around the y -axis, while σ_z and σ_x refer to reflection symmetries through the z -axis and the x -axis, respectively.

A more detailed discussion pertaining to the properties of symmetry, reciprocity and angular scattering will be presented at the conference.

REFERENCES

- [1] K. Achouri and C. Caloz, "Design, concepts, and applications of electromagnetic metasurfaces," *Nanophotonics*, vol. 7, no. 6, pp. 1095–1116, 2018.
- [2] K. Achouri, B. A. Khan, S. Gupta, G. Lavigne, M. A. Salem, and C. Caloz, "Synthesis of electromagnetic metasurfaces: principles and illustrations," *EPJ Applied Metamaterials*, vol. 2, p. 12, 2015.
- [3] K. Achouri, M. A. Salem, and C. Caloz, "General metasurface synthesis based on susceptibility tensors," *IEEE Trans. Antennas Propag.*, vol. 63, no. 7, pp. 2977–2991, Jul. 2015.
- [4] Y. Vahabzadeh, N. Chamanara, K. Achouri, and C. Caloz, "Computational Analysis of Metasurfaces," *IEEE J. Multiscale and Multiphys. Comput. Techn.*, vol. 3, pp. 37–49, 2018.
- [5] K. Achouri and O. J. Martin, "Influence of reciprocity, symmetry and normal polarizations on the angular scattering properties of bianisotropic metasurfaces," *arXiv preprint arXiv:1808.08196*, 2018.